Columbia University
in the City of New York

LAMONT GEOLOGICAL OBSERVATORY
PALISADES, NEW YORK

Technical Report on Seismology No. 33

Two-Dimensional Model Seismology

LAMONT GEOLOGICAL OBSERVATORY

(Columbia University)

Palisades, New York

* * *

Technical Report No. 33

CU-43-53-AF 19(122)441 - GEOL.

Two-Dimensional Model Seismology

by

Jack Oliver, Maurice Ewing, and Frank Press

The research reported in this document has been made possible through support and sponsorship extended by the Geophysics Research Division of the Air Force Cambridge Research Center under Contract AF 19(122)441. It is published for technical information only and does not represent recommendations or conclusions of the sponsoring agency.

November 1953

ABSTRACT

The solutions of many problems in seismology may be obtained by means of ultrasonic pulses propagating in small scale models. Thin sheets, serving as two dimensional models, are particularly advantageous because of their low cost, availability, ease of fabrication into various configurations, lower energy requirements and appropriate dilatational to shear velocity ratios. Four examples are presented: flexural waves in a sheet, Rayleigh waves in a low velocity layer overlying a semi-infinite high velocity layer, Rayleigh waves in a high velocity layer overlying a semi-infinite low velocity layer, and body and surface waves in a disk.

INTRODUCTION

In recent years investigators in both the commercial and academic fields have attacked the problems of elastic wave propagation by studying waves of ultrasonic frequencies traveling through small scale three dimensional models, and a few papers have been published on the subject [3, 6, 7]. Although promising results were obtained, widespread application of the method to significant problems has been slow, chiefly because of the difficulties in procuring suitable model materials and in the fabrication of desirable configurations. This paper describes the use of two dimensional models, which virtually eliminates these and other difficulties without detracting from the usefulness of the method in a great majority of cases.

The models take the form of thin sheets and the propagation takes place along directions lying in the plane of the sheet. In practice these sheets are generally 1/16" thick, and only wavelengths long compared to this thickness are employed.

THEORY

We wish to determine the propagation velocities of dilatational and shear waves in a thin plate and of Rayleigh waves on the edge of a thin plate. We restrict ourselves to waves in which the particle motion is symmetrical about the median plane of the plate, thus excluding any type of wave motion which involves bending of the thin plate.

For a perfectly elastic isotropic material, the equations of motion, neglecting external forces, are in the notation of Bullen[1].

$$(1) \qquad \rho f_i = \frac{\partial p_{ij}}{\partial x_j}$$

where ρ is the density, f_i the acceleration, p_{ij} the stress in the j th direction on the face normal to the i th axis, and x_i the co-ordinates. A summation convention is observed whereby if any suffix occurs twice in single term it is to be put equal to 1, 2 and 3 in turn and the results added.

The stresses are given by

$$(2a) \qquad p_{ij} = \lambda \theta \delta_{ij} + 2\mu e_{ij} \qquad \text{where} \quad \begin{matrix} \delta = 1 \text{ if } i = j \\ \delta = 0 \text{ if } i \neq j \end{matrix}$$

and where λ and μ are Lamé's constants and

$$e_{ij} = \frac{1}{2}\left(\frac{\partial u_j}{\partial x_i} + \frac{\partial u_i}{\partial x_j}\right)$$

where the u's are the displacements and

$$\theta = e_{11} + e_{22} + e_{33} = \frac{\partial u_1}{\partial x_1} + \frac{\partial u_2}{\partial x_2} + \frac{\partial u_3}{\partial x_3}$$

We restrict ourselves to a plate which is thin compared to the wavelengths which we will study. The 3 axis is taken perpendicular to the plane of the plate. The stresses then become

(2b) $$\phi_{11} = \lambda\theta + 2\mu e_{11}$$

(2c) $$\phi_{22} = \lambda\theta + 2\mu e_{22}$$

(2d) $$\phi_{33} = \lambda\theta + 2\mu e_{33} = 0$$

(2e) $$\phi_{12} = \phi_{21} = 2\mu e_{12}$$

(2f) $$\phi_{31} = \phi_{32} = \phi_{13} = \phi_{23} = 0$$

from (2d) $$\lambda\theta = \lambda(e_{11} + e_{22} + e_{33}) = -2\mu e_{33}$$

$$e_{33} = -\frac{\lambda}{\lambda + 2\mu}(e_{11} + e_{22})$$

(2g) $$\theta = \frac{2\mu}{\lambda + 2\mu}\tau \qquad \text{where} \quad \tau = \frac{\partial u_1}{\partial x_1} + \frac{\partial u_2}{\partial x_2}$$

Substituting (2) into (1)

(3) $$\rho \frac{\partial^2 u_i}{\partial t^2} = \left(\frac{2\mu\lambda}{\lambda + 2\mu} + \mu\right)\frac{\partial \tau}{\partial x_i} + \mu D^2 u_i$$

where

$$D^2 = \frac{\partial^2}{\partial x_1^2} + \frac{\partial^2}{\partial x_2^2}$$

The corresponding equation for an infinite solid is

$$\rho \frac{\partial^2 u_i}{\partial t^2} = (\lambda+\mu)\frac{\partial \theta}{\partial x_i} + \mu \nabla^2 u_i$$

Differentiate both sides of (3) with respect to x_i (this involves separate differentiations with i =1 and 2 and adding the results), to obtain the dilatational wave equation

$$(4) \qquad \rho \frac{\partial^2 \theta}{\partial t^2} = \frac{4\mu(\lambda+\mu)}{\lambda+2\mu} D^2\theta$$

Equation (4) checks the velocity given by Lamb for dilatational waves in a plate, i. e.

$$(5) \qquad V_\phi = \left[\frac{4\mu(\lambda+\mu)}{\rho(\lambda+2\mu)}\right]^{1/2}$$

Take the curl (two dimensional) of (3) and we get

$$(6) \qquad \rho \frac{\partial^2}{\partial t^2}(\mathrm{curl}\, u_i) = \mu D^2(\mathrm{curl}\, u_i)$$

Thus the shear wave velocity is the same as in an infinite solid,

i. e. $$\beta = \left(\frac{\mu}{\rho}\right)^{1/2}$$

We now consider a thin plate which occupies the 1, 2 plane from x_2=0 to $x_2 = +\infty$. Let

$$(7) \qquad u_1 = \frac{\partial \phi}{\partial x_1} + \frac{\partial \psi}{\partial x_2} \qquad u_2 = \frac{\partial \phi}{\partial x_2} - \frac{\partial \psi}{\partial x_1}$$

then

$$D^2\phi = \theta$$

$$D^2\psi = \frac{\partial u_1}{\partial x_2} - \frac{\partial u_2}{\partial x_1}$$

(8) Where ϕ and ψ satisfy

$$\frac{\partial^2 \phi}{\partial t^2} = V_\phi^2 \nabla^2 \phi \qquad \frac{\partial^2 \psi}{\partial t^2} = \beta^2 \nabla^2 \psi$$

Choose plane wave solutions of the form

(9a)
$$\phi = A e^{ik(-r x_2 + x_1 - ct)}$$
$$\psi = B e^{ik(-s x_2 + x_1 - ct)}$$

(9b) where $r = \left(\frac{c^2}{V_\phi^2} - 1\right)^{1/2}$, $s = \left(\frac{c^2}{\beta^2} - 1\right)^{1/2}$

C is the velocity of propagation of constant phase in the x_1 direction, and k is the wave number. Thus the wavelength in the x_1 direction, ℓ is given by $\ell = \frac{2\pi}{k}$ and the period T by $T = \frac{2\pi}{kc}$

(10) At the free edge $x_2 = 0$, $\sigma_{12} = \sigma_{22} = 0$

using (2c, (2g), (7), (9) and (10) we get

(11) $$\left[V_\phi^2(1+r^2) - 2\beta^2\right]A + 2\beta^2 s B = 0$$

from (2e), (7), (9) and (10) we get

(12) $$2rA + (1-s^2)B = 0$$

Eliminating A and B from (11) and (12) and using (9b)

(13) $$\left(2 - \frac{c^2}{\beta^2}\right)^2 = 4\left(1 - \frac{c^2}{V_\phi^2}\right)^{1/2}\left(1 - \frac{c^2}{\beta^2}\right)^{1/2}$$

This is identical with the equation for Rayleigh waves on the surface of a SEMI-infinite solid with the exception that the plate dilatational velocity replaces the infinite solid dilatational velocity. It is clear that no difficulties will arise in more complicated cases. Thus most of the problems on propagation of plane waves in a stratified earth may be

related to the two dimensional models by simply replac ing α by V_p.

EQUIPMENT AND TECHNIQUES

The principal features of the apparatus and procedure are described here briefly. The transmitting and receiving equipment is adapted from similar equipment in use in several laboratories, but the use of thin plates for construction of the models is apparently novel.

A block diagram of the equipment is shown in Fig. 1. Electrical pulses of approximately 15 microsecond duration are applied to the transmitter, a small piezoelectric element in contact with the model. This transducer delivers an acoustical pulse, shown as traced from the seismogram in Fig. 2, to the model. The resulting acoustical energy arriving at various points on the model is detected by a similar transducer, amplified, and then displayed on the cathode ray oscilloscope. The pulse repetition rate is adjustable from 2 to 100 pulses per second. The oscilloscope sweep is triggered at a fixed time interval ahead of the pulse so that a standing wave pattern, including the time break, is observed. The basic timing unit which initiates the trigger pulses for both the oscilloscope and the pulse also supplies timing markers at convenient intervals. The resulting pattern on the oscilloscope is then photographed by a Polaroid Land camera and the miniature seismogram is obtained immediately.

The transmitting transducer is a barium titanate cylinder 1/10" thick, 1/4" diameter. To prevent internal reflections in the source mount, the transducer is backed by a long aluminum rod of the same diameter. The part of the pulse energy that enters the backing and then reflects from the end of the rod back toward the source is too late and too greatly attenuated to confuse the seismogram. Difficulties due to free oscillations or "ringing" of the source are avoided by utilizing a frequency range that is below the ringing frequency of the transducer. The receiving transducer is also of barium titanate 1/25" thick and 3/32" diameter and is mounted in a similar but less elaborate manner. The smaller thickness further improves the reduction of ringing.

The electronic equipment is currently under improvement and will be thoroughly described in a later report. The present unit delivers a pulse of about 1000-2000 volts to the source crystal. The voltage amplification of the receiving unit is less than 100,000.

The two dimensional models are usually built in the form of disks. These are particularly advantageous for the study of surface waves on the edge of the disk since there are no reflections of the surface waves and since a very long path may be obtained by using the multiple trips around a relatively small disk. The curvature of the disk may be made small compared to a wavelength so that the usual surface wave equations for flat-lying strata will be applicable.

with the slight modification of the dilatational wave velocity, or it may be made larger for studying the effect of sphericity of the earth upon long period surface waves. The body phases of earthquake seismology may be studied in the usual manner very conveniently. Any degree of complexity in the layering may be obtained by means of concentric rings of various materials glued together in the desired relation. The diameters of the disks used in this study are about 20". The thickness is at present standardized at 1/16". This is small compared to all the wavelengths involved so that there is no dispersion due to finite disk thickness. For some types of problems shapes other than the circular might be desirable, e.g. refraction and reflection problems of seismic prospecting may be studied by constructing a cross section of the configuration in question. Table 1 lists the materials that have been sampled to date with the compressional, shear and Rayleigh velocities.

The disks are held in position by three rubber-covered supports which touch the disks at three points on the periphery (Plate 1). Experiments show that for a disk of this thickness the supports do not affect the surface wave propagation appreciably. The disk is mounted concentric with a graduated ring on which the receiver travels, allowing accurate measurement of all arc distances. The transmitting transducer is set at an arbitrary zero which may be determined accurately by running profiles from the transducer in both directions. A plot of the dilatational wave travel times vs. distance

immediately gives the zero of the transmitted pulse in both time and distance.

COMPARISON OF TWO AND THREE DIMENSIONAL MODELS

Two dimensional models (2-D) have the following advantages over three dimensional (3-D) models.

1. The materials are far less expensive. 3-D models are usually constructed of some material which can be poured, e. g. wax, concrete, tars, or various chemical setting cements, or of some material which can be purchased in large slabs, e. g. limestone, marble, etc. All of these are expensive and become increasingly difficult to handle when layered media are desired. It is particularly difficult to pour materials in large blocks and maintain homogeneity throughout. The 2-D models, on the other hand, may be constructed of any material which can be bought in 1/16" sheets. This includes most metals and alloys and many types of plastics, fibers, etc. They are not prohibitively expensive and are generally far more homogeneous than poured materials.

2. The fabrication is greatly simplified. Layered configurations may be built up from concentric rings, easily cut to accurate specifications on a large lathe. Almost any sort of hard glue may be used as a binding agent.

3. Storage is simplified, a drawer of a map case may be used for storage of a large number of 2-D models. 3-D models

frequently require about 50 sq. feet of floor space for each model.

4. The energy requirements are greatly diminished in the 2-D model. For body waves the intensity varies as $\frac{1}{R}$ as opposed to $\frac{1}{R^2}$ in the 3-D case. Surface waves undergo no geometrical attenuation instead of the $\frac{1}{R}$ variation in the 3-D case. This is a tremendous advantage as it allows the use of pulses of 1000 volts or less as opposed to 5000-10,000 volts in the 3-D case. Similarly lower gains may be used in the amplifying system which permits use of a simple receiving circuit.

5. Most materials commercially available do not make good models of rock because Poisson's ratio is too large, usually about .33 as opposed to about .25 for rocks. In the 2-D model the dilatational wave velocity is altered (see theory) so that a pseudo-Poisson's ratio (the same relation of the dilatational and shear velocities as for Poisson's ratio) now falls in the range appropriate to rocks (see Table 1).

6. Multiple trips around the disk by the surface waves may be used to give large path distances. The present paper includes waves that have made 2 1/2 trips (about 13 feet) but waves have been observed that have made 7 1/2 complete circuits (about 40 feet). Although a similar scheme might be followed three-dimensionally by using a sphere, the construction of spheres, particularly with concentric layers, is very difficult.

The multiple paths also provide a means of measuring attenuation that is free of instrument calibration and differences in coupling of the model to the transducer. This approach is identical to that used in the measurement of the absorption coefficient of the mantle by means of long Rayleigh waves [2].

At present 3-D models are necessary only when one or more layers of a stratified configuration is a liquid or when it is desirable to model three dimensional effects such as reflections not in the vertical plane of the shot and detector, as might be encountered in seismic prospecting.

EXAMPLES

Flexural Waves. The experimental model for studying the propagation of flexural waves in a plate, as worked out by Lamb,[4] was a ring cut from 24 ST Aluminum sheet, 1/16" thick. The outside diameter $2R_2$ of the ring was 19.112 inches and the inside diameter $2R_1$, 1/2" less. Radial motions of the ring were investigated as the 2-D analog of ordinary flexural waves. Figure 4 is a tracing of the oscillogram obtained with the receiver at the antipodes of the source. At this point there is constructive interference between the waves arriving from opposite directions. The first arrival following the time break corresponds to a dilatational wave through the ring. The first dispersive train of flexural waves corresponds to R_1 and R_2, the second to R_3 and R_4 etc., where

the R's with subscripts are used in the same sense as in earthquake seismology. The values obtained from the experimental data are plotted as the small circles of Fig. 4.

The theoretical equations for wave motion in an elastic plate in a vacuum were presented by Lamb[4]. The dispersion of flexural waves is determined by his period equation for asymmetrical motion. In our notation this equation takes the form

$$\frac{\tanh \frac{kh}{2}\left(1-\frac{c^2}{\beta^2}\right)^{1/2}}{\tanh \frac{kh}{2}\left(1-\frac{c^2}{\alpha^2}\right)^{1/2}} = \frac{\left(2-\frac{c^2}{\beta^2}\right)^2}{4\left(1-\frac{c^2}{\alpha^2}\right)^{1/2}\left(1-\frac{c^2}{\beta^2}\right)^{1/2}}$$

where h is the layer thickness.

To adapt this to our 2-D models we need only replace α by V_g and h by $R_2 - R_1 \equiv H$ Group velocity is obtained from the well known formula

$$U = C + \kappa H \frac{\partial C}{\partial \kappa H}$$

A family of theoretical curves of group velocity vs. period computed with the constants for 24 ST Aluminum alloy is shown in Fig. 4. Thickness is the parameter and very close agreement with the observed points is evident. Thus we have a good check on both the theory and the experimental method.

Slight complications have arisen due to the shape of the source pulse, in particular the later origin times of the longer periods. This difficulty may be completely circumvented by measuring arrival times of each period on successive trips around the ring and calculat-

ing the group velocity over the interval. The points of Fig. 4 were obtained by this method. If the initial rise of the source is used as a time break, a maximum error of 2% in the velocity might result. This effect is interesting and will be the subject of future study but it does not affect the present results.

Rayleigh Waves - Low Velocity over High Velocity. The most common configuration in nature which produces dispersion in Rayleigh waves is comprised of a low velocity layer over a high velocity semi-infinite layer. Lee[5] presented the theoretical equations for this case. His period equation is

$$\xi\eta' = \xi'\eta$$

where

$$\xi = \left(2-\frac{c^2}{\beta^2}\right)\left[\left(\frac{c^2}{\beta'^2}\frac{\mu'}{\mu}-\gamma\right)\cos kh\eta_1+\frac{\eta_1'}{\eta_1}\left(\frac{c^2}{\beta^2}+\gamma\right)\sin kh\eta_1\right]$$
$$+2\eta_2\left[\eta_1'\gamma\sin kh\eta_2-\frac{1}{\eta_2}\left(\frac{c^2}{\beta'^2}\frac{\mu'}{\mu}-\gamma-\frac{c^2}{\beta^2}\right)\cos kh\eta_2\right]$$

$$\xi' = \left(2-\frac{c^2}{\beta^2}\right)\left[\eta_2'\gamma\cos kh\eta_1+\frac{1}{\eta_1}\left(\frac{c^2}{\beta'^2}\frac{\mu'}{\mu}-\gamma-\frac{c^2}{\beta^2}\right)\sin kh\eta_1\right]$$
$$+2\eta_2\left[\left(\frac{c^2}{\beta'^2}\frac{\mu'}{\mu}-\gamma\right)\sin kh\eta_2-\frac{\eta_2'}{\eta_2}\left(\frac{c^2}{\beta^2}+\gamma\right)\cos kh\eta_2\right]$$

$$\eta = \left(2-\frac{c^2}{\beta^2}\right)\left[\eta_1'\gamma\cos kh\eta_2-\frac{1}{\eta_2}\left(\frac{c^2}{\beta'^2}\frac{\mu'}{\mu}-\gamma-\frac{c^2}{\beta^2}\right)\sin kh\eta_2\right]$$
$$+2\eta_1\left[\left(\frac{c^2}{\beta'^2}\frac{\mu'}{\mu}-\gamma\right)\sin kh\eta_1-\frac{\eta_1'}{\eta_1}\left(\frac{c^2}{\beta^2}+\gamma\right)\cos kh\eta_1\right]$$

$$\eta' = \left(2-\frac{c^2}{\beta^2}\right)\left[\left(\frac{c^2}{\beta'^2}\frac{\mu'}{\mu}-\gamma\right)\cos kh\eta_2+\frac{\eta_2'}{\eta_2}\left(\frac{c^2}{\beta^2}+\gamma\right)\sin kh\eta_2\right]$$
$$+2\eta_1\left[\eta_2'\gamma\sin kh\eta_1-\frac{1}{\eta_1}\left(\frac{c^2}{\beta'^2}\frac{\mu'}{\mu}-\gamma-\frac{c^2}{\beta^2}\right)\sin kh\eta_1\right]$$

$$\gamma = 2\left(\frac{\mu'}{\mu} - 1\right)$$

and

$$\eta_1 = \left(\frac{c^2}{\alpha^2} - 1\right)^{1/2} \qquad \eta_2 = \left(\frac{c^2}{\beta^2} - 1\right)^{1/2}$$

$$\eta_1' = \left(1 - \frac{c^2}{\alpha'^2}\right)^{1/2} \qquad \eta_2' = \left(1 - \frac{c^2}{\beta'^2}\right)^{1/2}$$

and the other symbols have the same meaning as before. Again we replace the α by Vp and the theoretical curves are shown in Fig. 5. The computed points are tabulated in Table 2. The constants were chosen to fit the case of Plexiglass overlying Panelyte. (See Table 1)

The disk was 19.522 inches in diameter with outside diameter of the outer ring 1/2" greater. Figure 6 is a record taken at $\Delta = 180^{\circ}$. Because of the small contrast between these two materials and the high attenuation in the plastic, more precision was obtained by using seismograms at several different Δ's rather than the one from the antipodes alone. As before, this eliminates the difficulty with the origin time of various periods in the pulse by making the velocity determination independent of pulse time. Fig. 5 shows the experimental results in good agreement with the theory.

The Panelyte is anisotropic having a velocity about 1 1/2% higher in one direction than in the perpendicular direction. This was not taken into account in the calculations and is a source of error in

the comparison with the theoretical curves. The points for the two longest periods both fall high. These long periods can only be distinguished in the dispersive train after a considerable length of path has been traversed. At that time the amplitudes are low and, in fact, the relative amplitudes of such periods are always low due to the pulse shape. Thus the accuracy of velocity measurement is reduced for these waves. Furthermore, it is possible that these waves may be long enough to be affected by the curvature of the disk. The discrepancy is in the proper direction, but this effect has not yet been studied. At most, however, the error is 2%.

Experiments in higher mode Rayleigh waves (shear modes) and on Stoneley waves are planned.

Rayleigh Waves - High Velocity over Low Velocity. The previous examples have shown a comparison of experimental data with theoretical curves. In both cases the theoretical calculations were relatively simple and within the range of an ordinary desk calculator. In the case of a high velocity layer over a semi-infinite low velocity stratum the computations increase greatly in complexity. On the other hand, there is no difficulty in modelling this case. Fig. 7 is a plot of the Rayleigh wave dispersion for the case of a ring of aluminum alloy overlying a disk of Plexiglass. Fig. 8 is a tracing of the seismogram at the antipodes. The ring of aluminum is the same as that used for the flexural waves. This configuration corresponds to a layer of rock

with elastic constants α =18,300 ft/sec and β =10,400 ft/sec overlying a semi-infinite layer with α =7,750 ft/sec β =4,500 ft/sec. The ratio of the densities is $\frac{\rho}{\rho_1} = \frac{2.77}{1.22}$. This is a fair approximation to the case of Palisades diabase overlying Triassic sandstones and shales along the west bank of the Hudson River. It is also similar to structure in the permafrost areas in the Arctic.

Because of the limited spectrum of the pulse only a portion of the complete dispersion curve is obtained. Other segments may be studied by varying the thickness of the layer.

Body and Surface Waves in Disks. The previous examples, all concerning surface waves, used wavelengths which were small enough compared to the curvature of the disks so that the waves were effectively traveling along flat surfaces. Disks were chosen merely as a convenient shape to work with because of the multiple paths and lack of surface wave reflections. However the disk as a two dimensional model of the earth also appears promising for the study of body waves. The seismograms of Fig. 9 were taken on a uniform plexiglass disk of diameter 10.75". Fig. 10 is a plot of the experimental points read from the records,compared with theoretical travel time curves based on velocities determined from the P arrivals. Poisson's ratio is taken as 1/4. Phases definitely identifiable are P, PP, S, PS and PPS, SS, and LR. At the larger Δ 's there is some difficulty in determining the exact arrival time and phase of the later arrivals due to overlap-

ping of other phases. The present picks for the later arrivals are nearly always late. Clearly, this can be avoided by the use of larger disks and future studies will be made on disks of at least twice this diameter. This should improve the resolution of phases and accuracy of the arrival times measurably.

The polarity of the first break of the Rayleigh wave changes with distance. Such is not the case for Rayleigh waves propagating along the straight edge of a plate, which rules out the possibility of selective absorption of the high frequencies as the cause. The change of polarity is possibly the result of the generation of the waves by the curved P and S wave fronts at the surface. The phenomenon is not understood at present.

Scaling to Related Problems. The dispersion curves of the preceding examples are presented in the dimensions as modeled. Scaling to other problems is a relatively simple matter, as can be seen from an inspection of the period equation for flexural waves or Rayleigh waves. Once a fixed relation is established between all the dilatational and shear velocities the equations may be solved for the ratio c/β or c/α and similarly v/β or v/α . Thus velocities may be scaled to any other problem for which the elastic constants have the same ratios merely by multiplying the measured velocities by the appropriate ratio $\frac{\beta'}{\beta}$ or $\frac{\alpha'}{\alpha}$. Similarly the period associated with a given phase and group velocity will vary directly with H, the layer thickness.

ACKNOWLEDGMENTS

The authors wish to acknowledge the assistance of many co-workers at the Lamont Geological Observatory. In particular, Mr. Charles Kershaw constructed all the electronic gear and designed the new components. Mr. James Dorman and Mr. Donald Schiller carried out the computations, and Mr. Louis Collyer built the mechanical parts of the apparatus.

The Carter Oil Company generously gave assistance in the design of circuits used, through Dr. Franklyn Levin, who participated in the seismic model work for that company.

REFERENCES

1. Bullen, K. E., "An Introduction to the Theory of Seismology", Cambridge University Press, 1947.

2. Ewing, M. and Frank Press, "An Investigation of Mantle Rayleigh Waves", in press Bull. Seis. Soc. Am.

3. Kaufman, S. and W. L. Roever, "Laboratory Studies of Transient Elastic Waves", Proceedings of Third World Petroleum Congress, The Hague, 1951. Section I, pp. 537-545.

4. Lamb, H., "On Waves in an Elastic Plate", Proc. Roy. Soc. Lond. A 93, p. 114, 1917.

5. Lee, A. W., "The Effect of Geological Structure on Microseismic Disturbances", Mon. Not. Roy. Ast. Soc. Geoph. Suppl. 3: 83-105, 1932.

6. Northwood, T. D. and D. V. Anderson, "Model Seismology", Bull. Seis. Soc. Am., 43: 239-246, July 1953.

7. Terada, T. and C. Tsuboi, "Experimental Studies on Elastic Waves (Parts I and II)", Tokyo Imperial University, Bull. Earthquake Res. Inst., 3: 55-65, 4: 9-20 (1927).

TABLE 1

MEASURED ELASTIC WAVE VELOCITIES AND DENSITIES

Material	Designation	Sample	Plate Dilatational Velocity V_p in ft/sec	Shear Velocity, β in ft/sec	Rayleigh Velocity V_r in ft/sec	Density ρ in gm/cc	Pseudo-Poisson's Ratio $\sigma = \frac{\frac{1}{2} - (\beta/V_p)^2}{1 - (\beta/V_p)^2}$	Remarks
Aluminum Alloy	24S-T4	Disk 1/16" x 10.56"	18,300	10,400	9,880	2.77	.26	
Plexiglass	Colorless, Transparent	Disk 1/16" x 10.75"	7,750	4,500	4,200	1.22	.25	
Panelyte	Grade 550	Disk 1/16" x 19.522"	10,650	6,000	5,600	1.44	.27	Anisotropic* 2%
Copper	Cold rolled	1/16" x 10.75"	13,000	7,500	6,900	9.03	.25	
Steel	"	"	17,850	10,650	9,700	7.78	.22	
Steel	Hot rolled	"	17,600	10,300	9,700	7.80	.24	
Brass	Half hard	"	12,500	7,000	6,500	8.34	.28	
Zinc		.052 x 10.75"	13,100	7,700	7,300	7.07	.24	
Vinyl Plastic	Phonograph record	1/16" x 11.875"	6,420	3,870	3,540	1.47	.21	

TABLE 1 (Cont'd.)

Material	Designation	Sample	Plate Dilatational Velocity V_p in ft/sec	Shear Velocity, in ft/sec	Rayleigh Velocity V_r in ft/sec	Density in gm/cc	Pseudo-Poisson's Ratio	Remarks
Fish paper	Franklin Fibre Lamitex	1/16" x 10.875"	8,970	5,490	5,110	1.14	.22	Anisotropic* 22%
Fibre	Franklin Hard Vulcanized	1/16" x 10.875"	8,650	5,270	4,900	1.06	.21	Anisotropic* 15%
Formica	Linen Laminate	1/16" x 10.75"	8,450	5,050	4,700	1.30	.24	Anisotropic* 7%

* For anisotropic materials slowest velocities are tabulated. These are generally perpendicular to the grain. For Panelyte the tabulated velocity is an average.

TABLE 2

Phase and group velocity vs KH for a layer with α =7750 ft/sec. β =4500 ft/sec. ρ =1.219 gm/cc overlying a semi-infinite layer with α =10,650 ft/sec. β =6000 ft/sec. ρ =1.436

Computed values		Values obtained graphically		
C in ft/sec.	KH	KH	U in ft/sec.	C in ft/sec.
5535	0	0	5535	5535
5500	.075	.05	5488	5510
5450	.203	.1	5449	5490
5400	.358	.2	5379	5453
5350	.550	.3	5323	5418
5300	.756	.4	5276	5388
5200	1.152	.5	5233	5362
5100	1.450	.75	5123	5302
5000	1.722	1.00	4978	5241
4900	1.955	1.25	4766	5168
4800	2.196	1.50	4543	5083
4700	2.425	1.75	4283	4977
4600	2.689	2.00	4020	4838
4400	3.392	2.25	3842	4973
4300	3.965	2.50	3685	4672
4200	5.107	2.90	3623	4528
		3.0	3626	4498
		4.0	3770	4296
		5.0	3886	4207

Plate 1. Model, Transducers and Oscilloscope

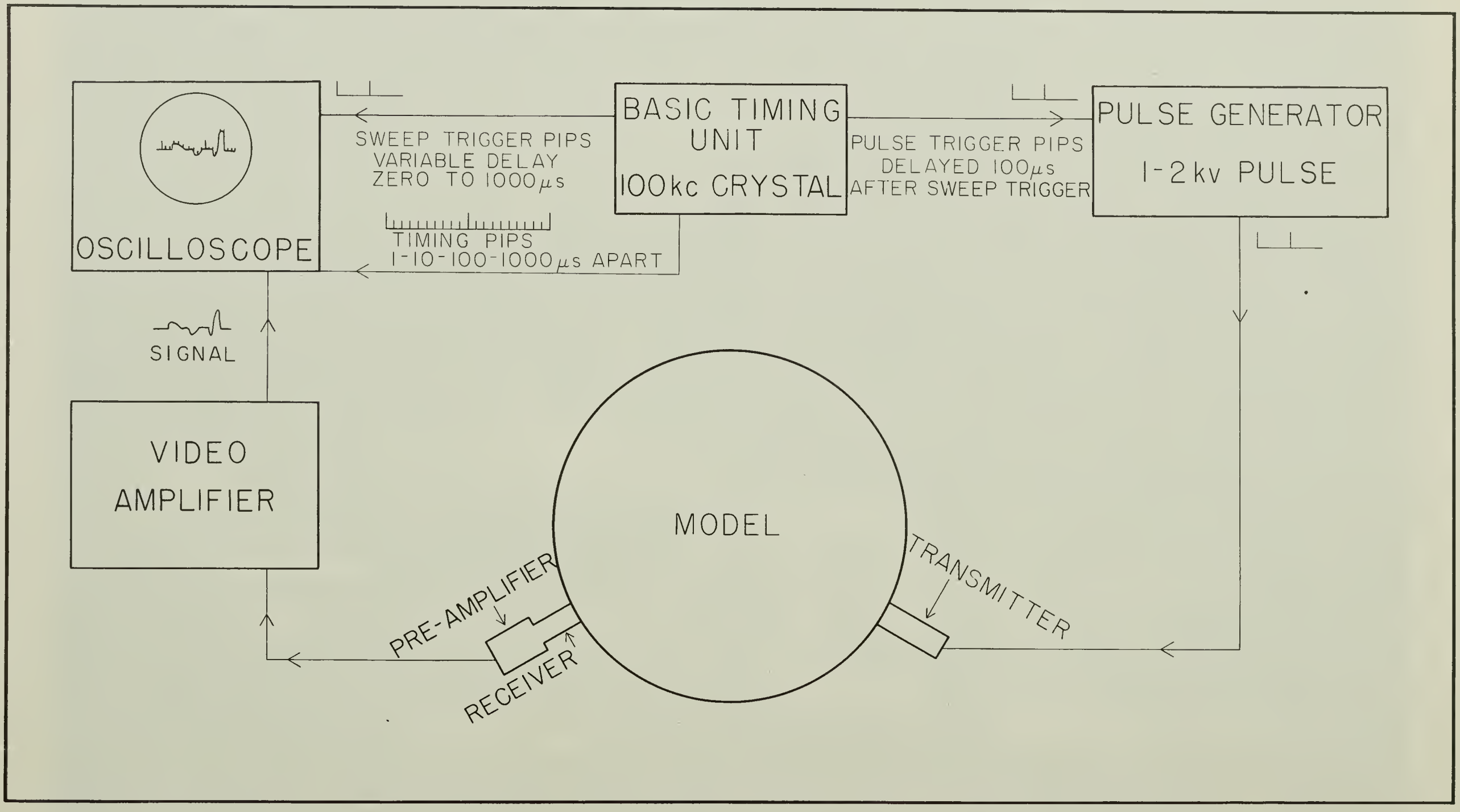

Figure 1. Block Diagram of Apparatus

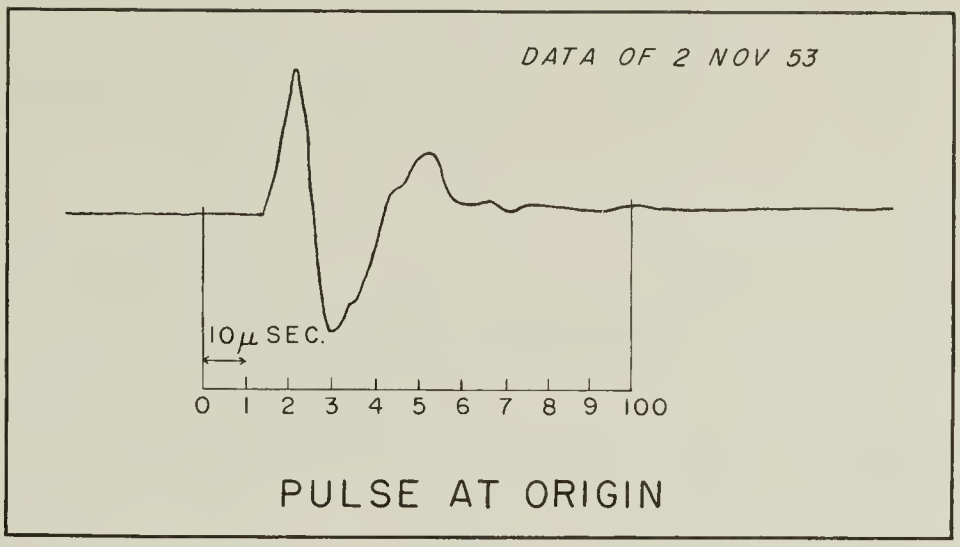

Figure 2. Pulse at Origin

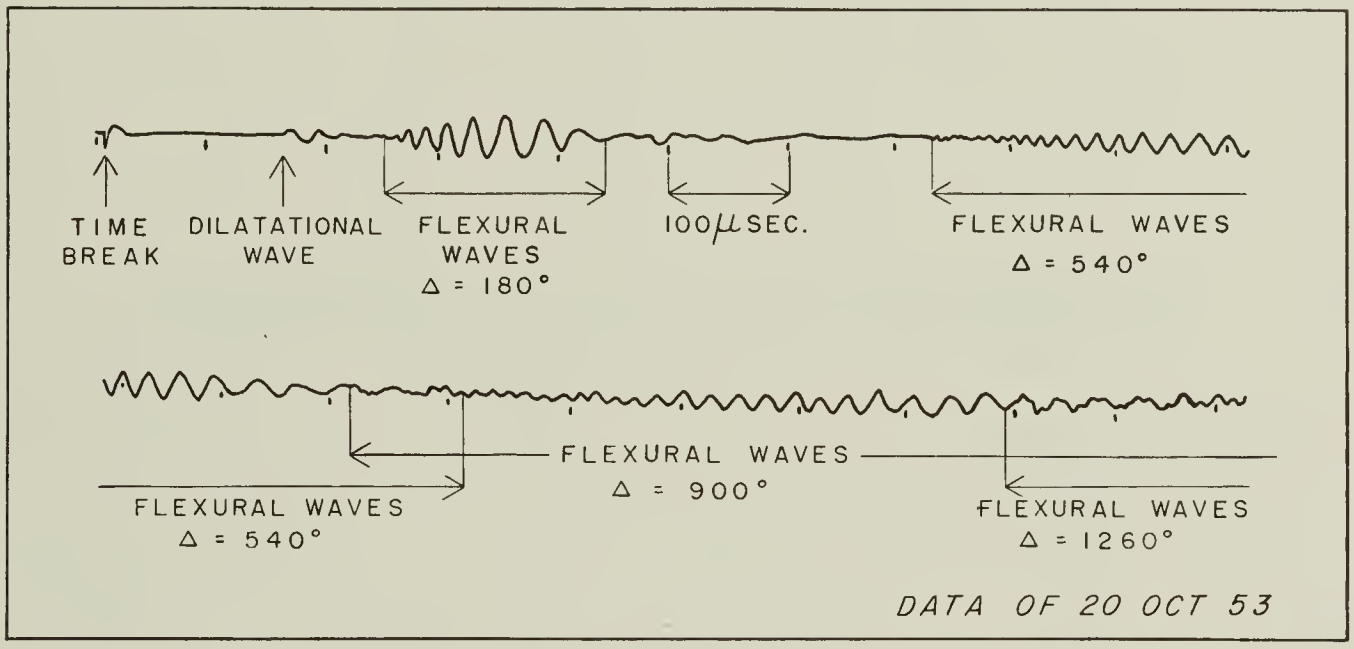

Figure 3. Seismogram - Flexural Waves

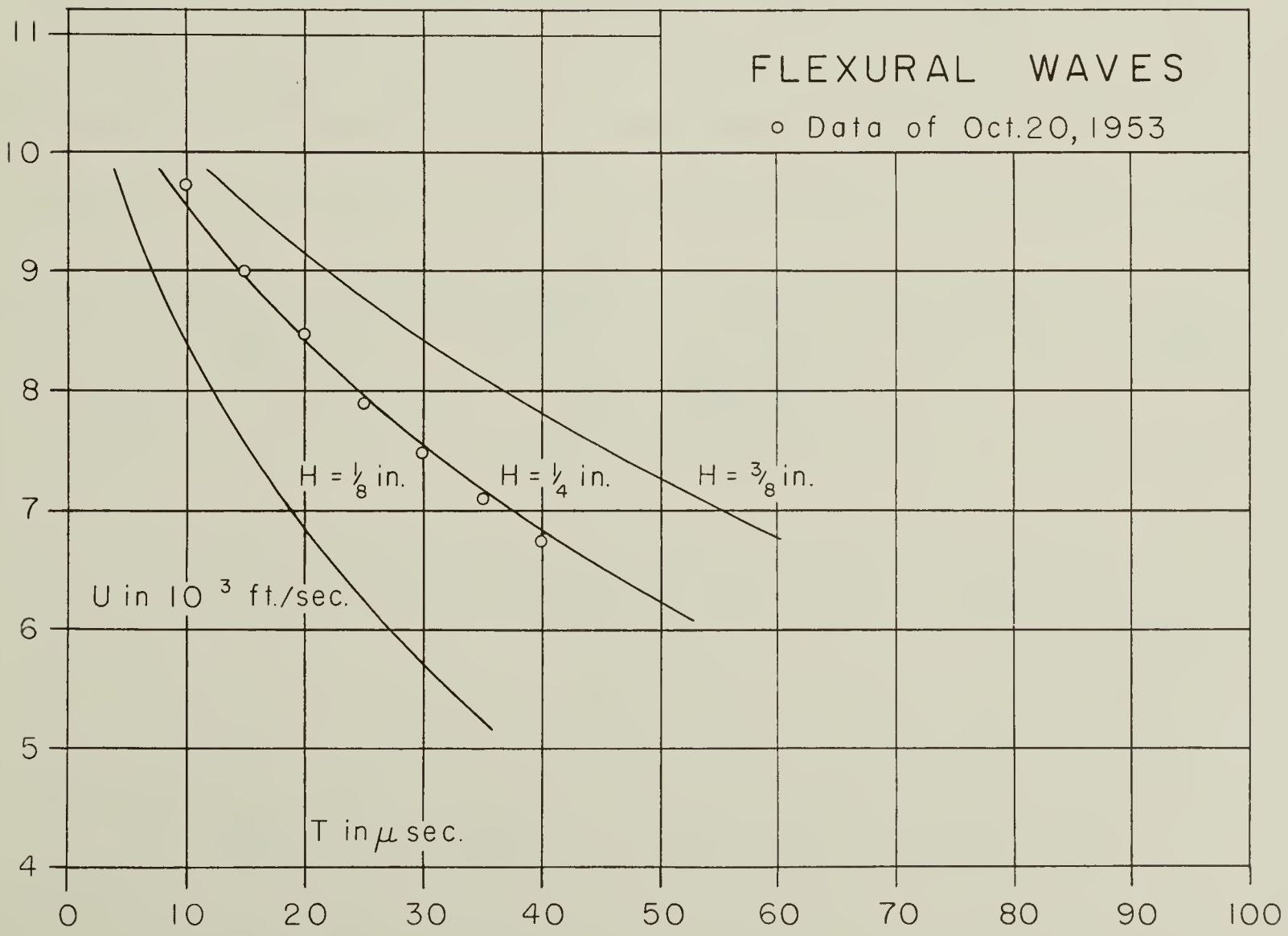

Figure 4. Flexural Wave Dispersion

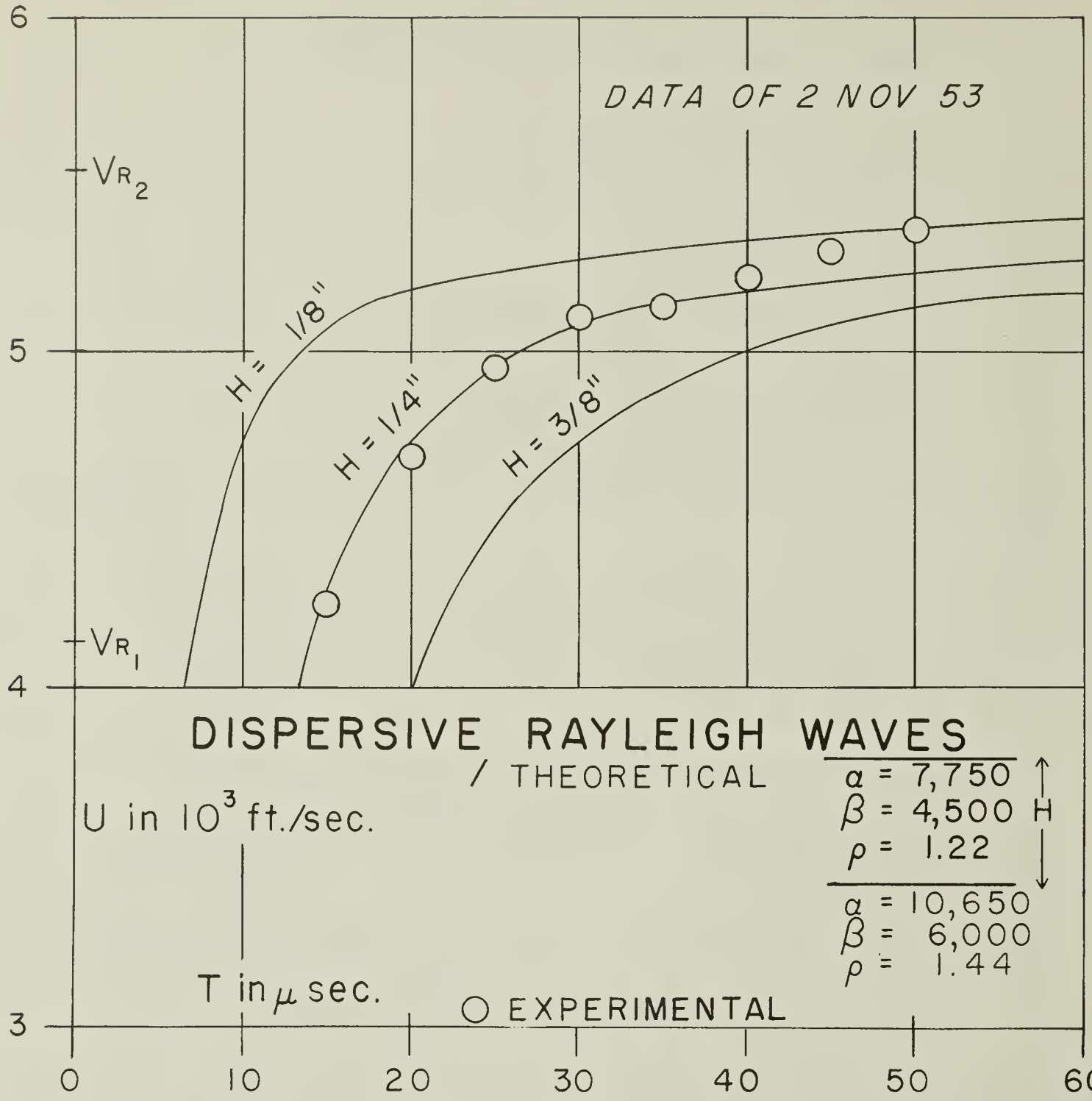

Figure 5. Rayleigh Wave Dispersion - Low Velocity/High Velocity

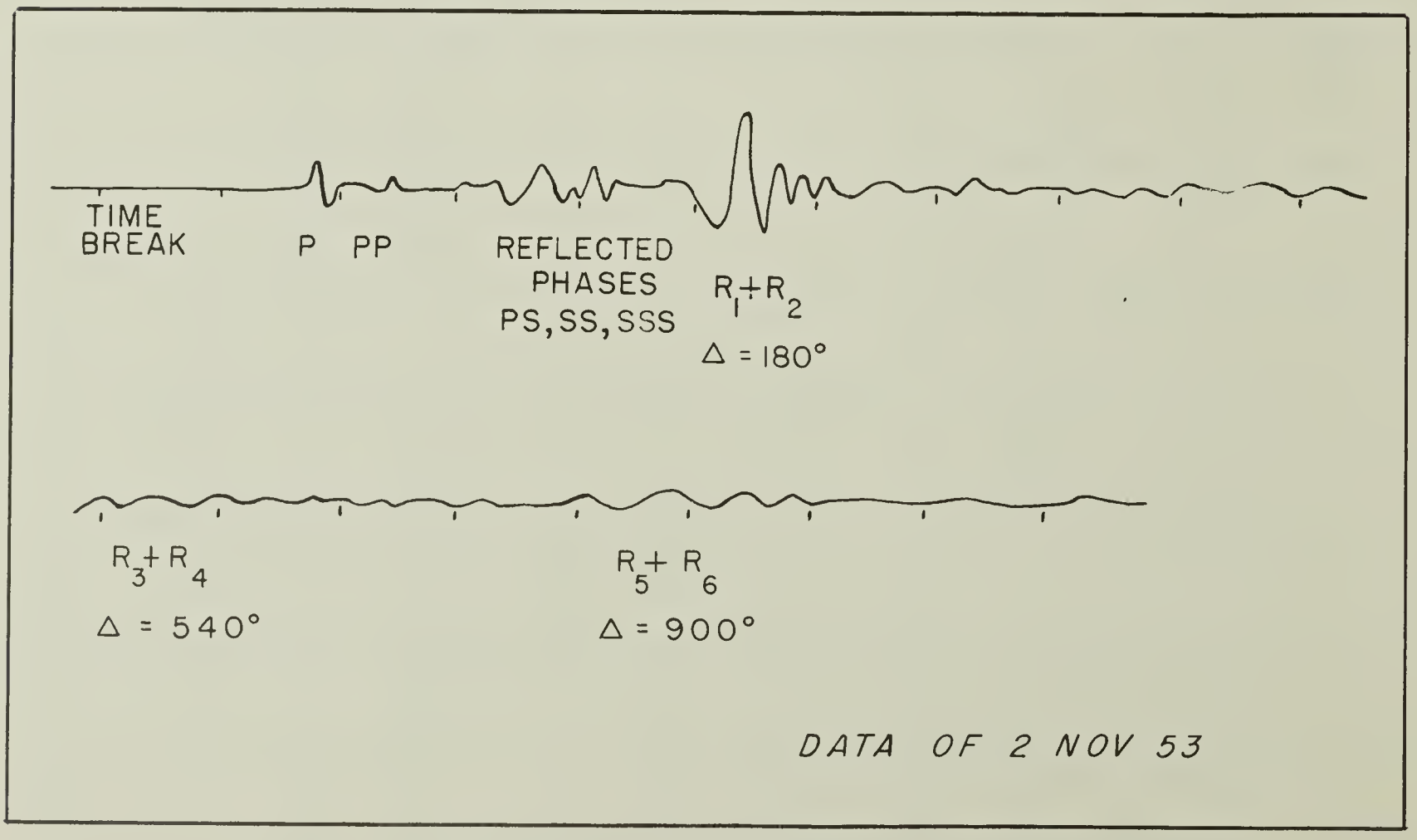

Figure 6. Seismogram - Low Velocity/High Velocity

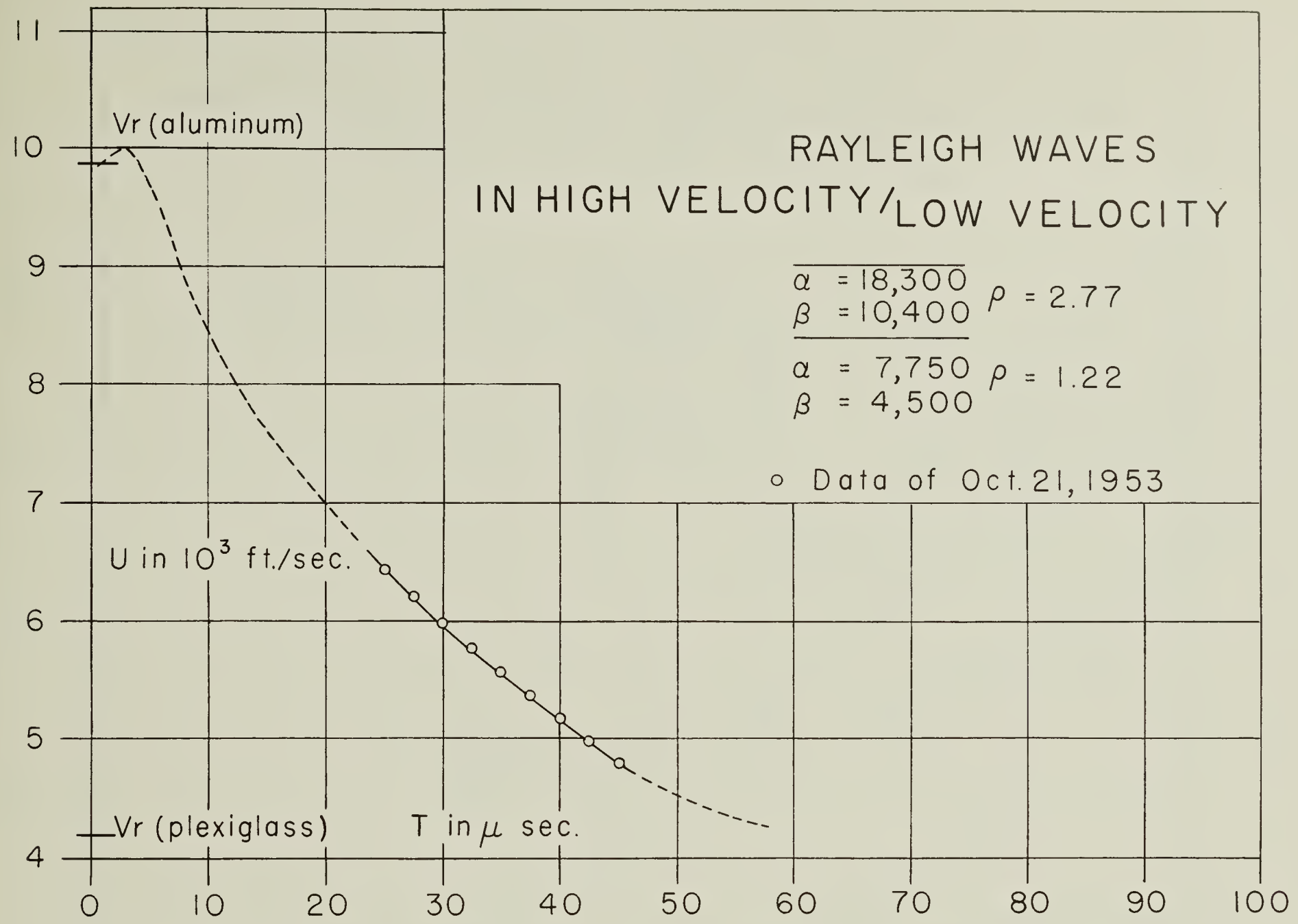

Figure 7. Rayleigh Wave Dispersion - High Velocity/Low Velocity

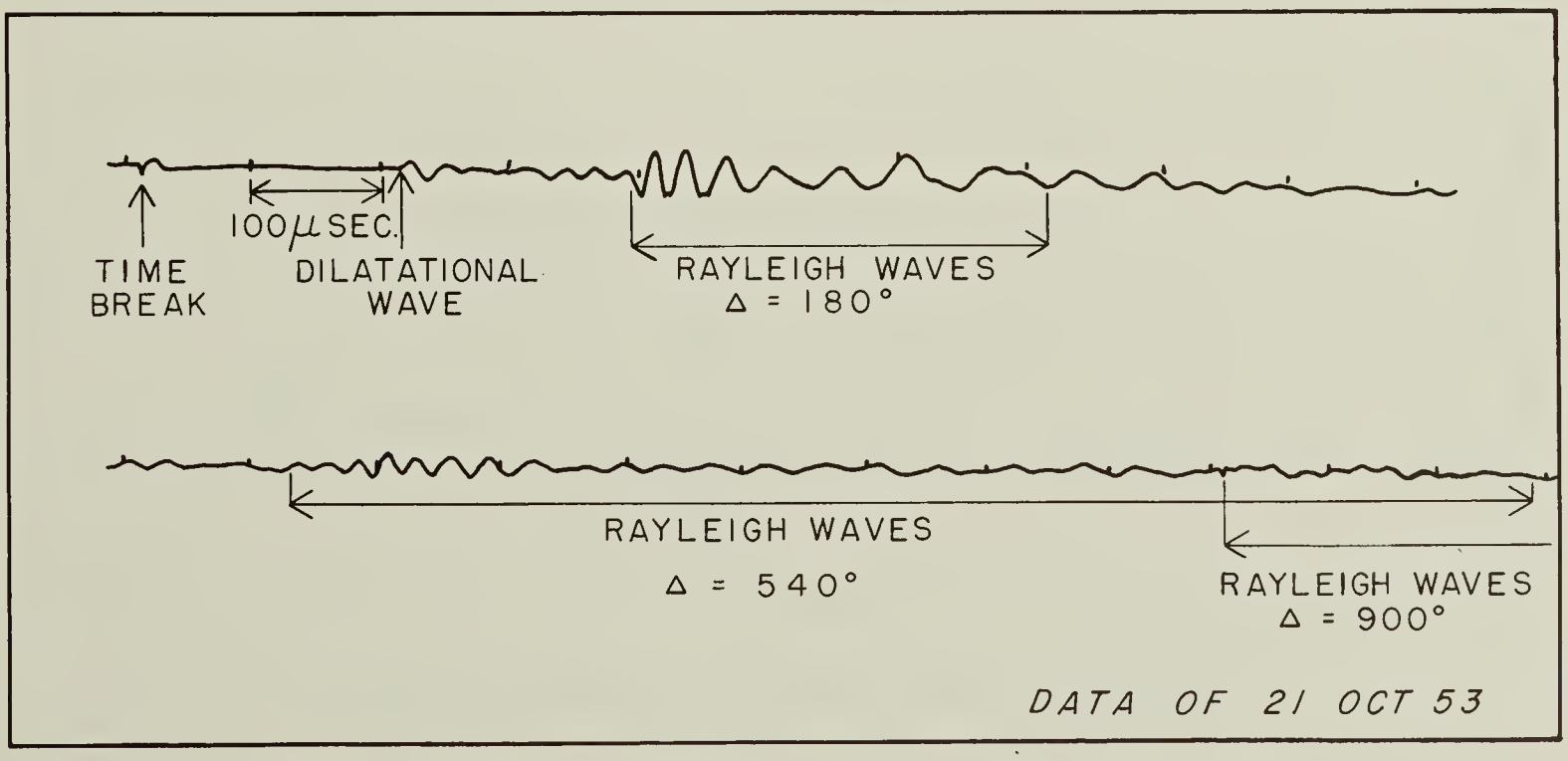

Figure 8. Seismogram - High Velocity/Low Velocity

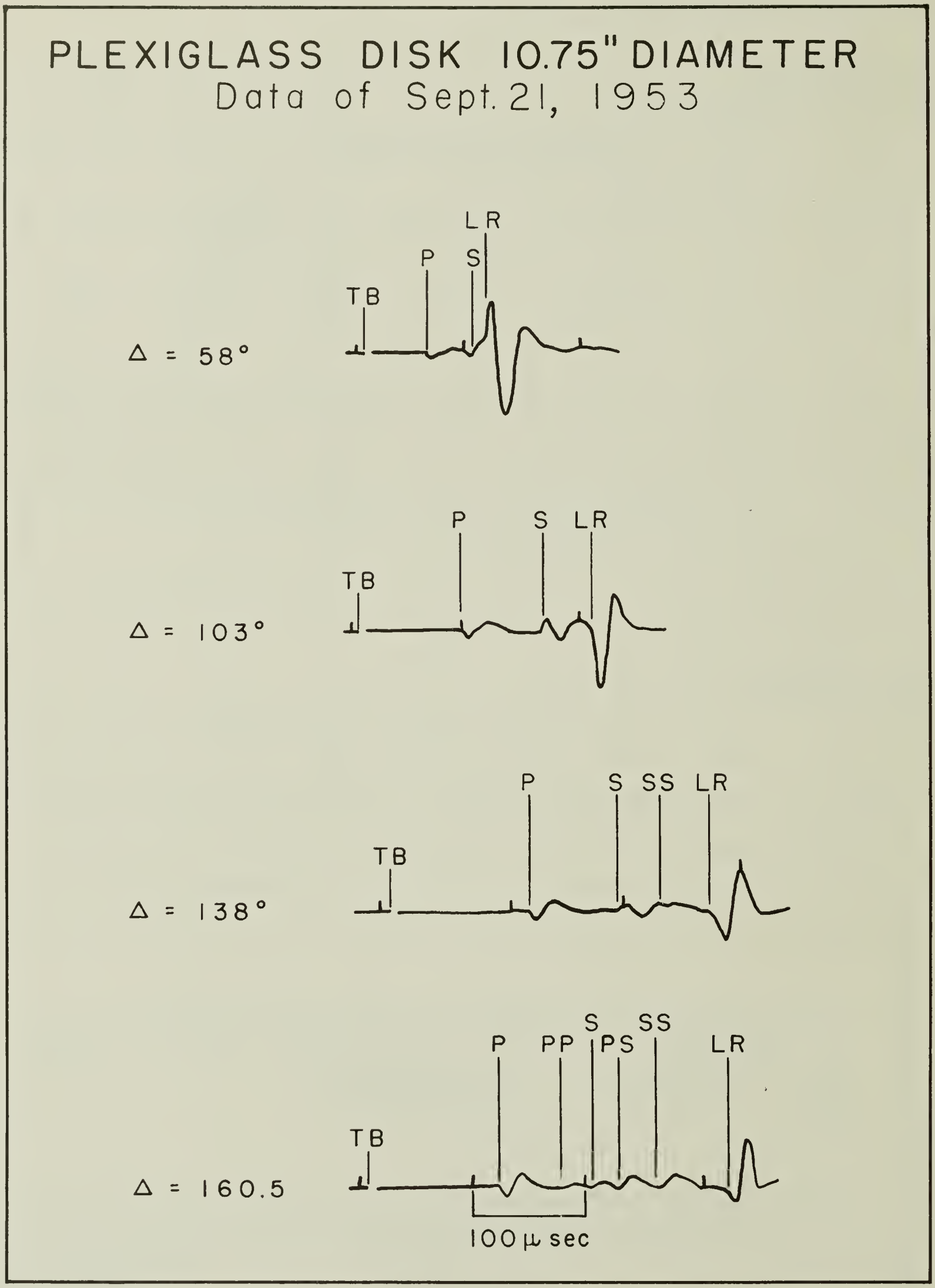

Figure 9. Seismogram - Plexiglass Disk

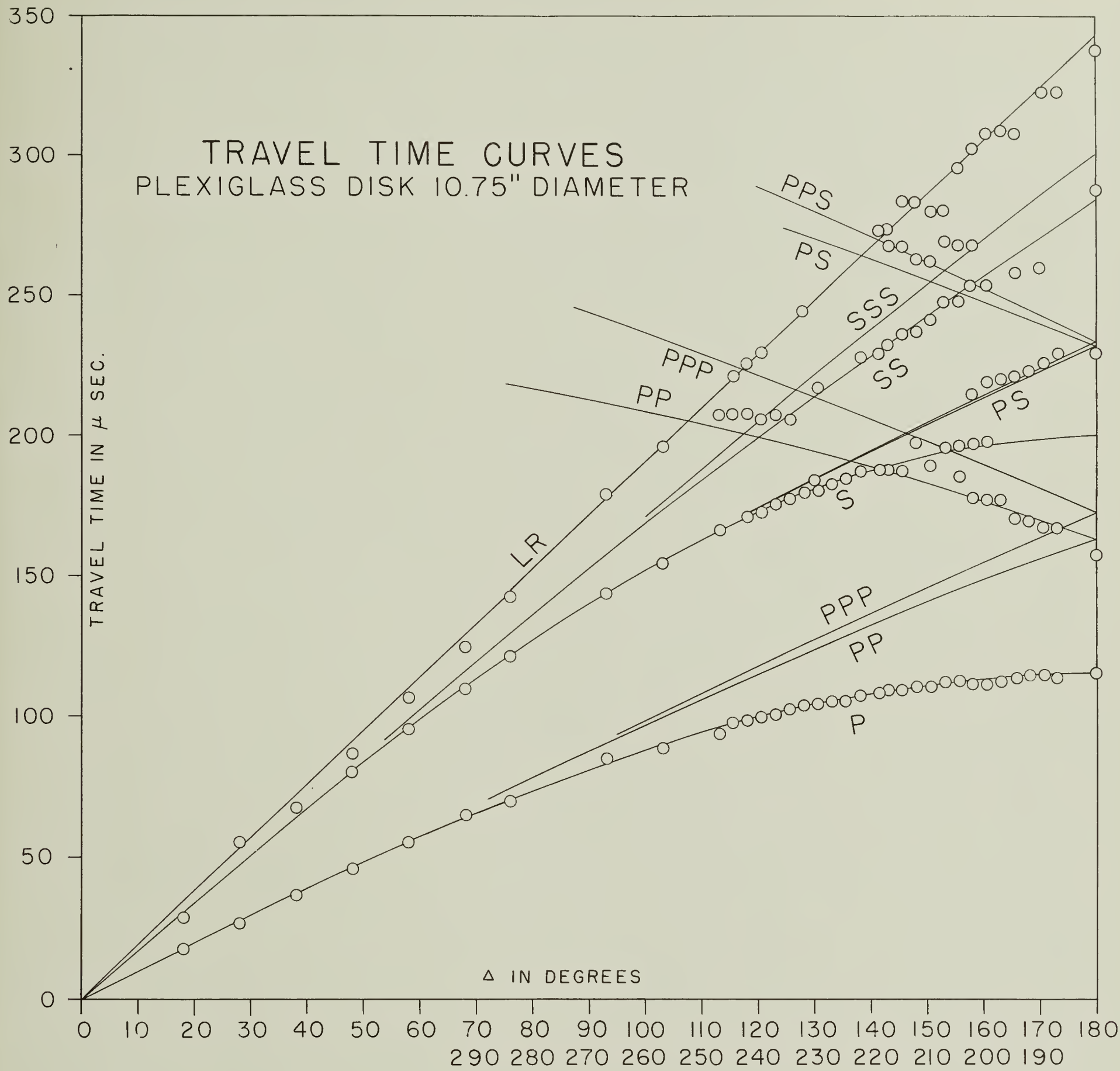

Figure 10. Travel Time Curves - Body & Surface Waves in a Disk